

NEAR-SPACE PASSIVE REMOTE SENSING FOR HOMELAND SECURITY: POTENTIAL AND CHALLENGES

Wen-Qin Wang^{a, b, *}

^a Lab 140, School of Communication and Information Engineering
University of Electronic Science and Technology of China, Chengdu, 610054, P. R. China

^b Beijing Key Lab of Spatial Information Integration and 3S Application, Peking University, Beijing 100871, China

* wqwang@uestc.edu.cn

Commission I , ThS-1

KEY WORDS: Near-space, homeland security, remote sensing, passive radar, monitoring, microwave imaging, disaster.

ABSTRACT:

Inspired by recent technical advances in near-space defined as the space region between 20km and 100km, which is above the storms and jet stream, and not constrained by the orbital mechanics of the satellite platforms or the high fuel consumptions of the airborne platforms, they can stay at a specific site almost indefinitely to provide a persistent coverage, this paper proposed the system concept of near-space remote sensing for homeland security applications. To the author's knowledge, I am the first author that proposes the concept of near-space remote sensing. This concept involves a passive radar receiver placed inside a near-space platform is in conjunction with the illuminator of opportunistic signals, so as to provide persistent mapping and monitoring of homeland. This paper deals with conceptual analysis, as opposed technological implementation. It is shown that the novel use of near-space platforms can provide the solutions that were thought to be out of reach for remote sensing scientists. The techniques and concepts discussed may be regarded as the Phase I work towards promising near-space remote sensing for homeland security applications.

1. INTRODUCTION

To protect civilian population, mass transmit, civil aviation, and critical infrastructure from terrorist attacks employing explosive devices, vast improvements in our current capability of protecting homeland security are required, so that efficiently neutralize these threats without significantly impacting our normal day-to-day activities. It appears that microwave remote sensing may play an important role in homeland security (Baker and Griffiths, 2005). The current spaceborne radar has playing an important role in remote sensing applications (Trouve et al., 2007); however, even as good as they are, they cannot provide a staring presence on a timescale of days, weeks, or months over a selected target or area of interest. Costing as much as billions of U. S dollars, or at least millions each with multiple satellites required to provide persistent coverage makes it prohibitively expensive. In contrast, conventional airplane cannot fly very high because there is insufficient oxygen to allow the engines to operate.

We thus have two identified gaps; one is the gap in capability and the other is the gap in the altitude between satellite and airplane. Fortunately, these two gaps can be simultaneously filled through the use of near-space platforms. Near-space defined as the region between 20km and 100km was a cultural blind spot – too high up for conventional aircrafts, but too low for LEO satellites. Inspired by recent advances in near-space technology, this paper presents the system concept of near-space remote sensing for homeland security applications. To the author's knowledge, I am the first author that proposes the concept of near-space remote sensing (Wang, 2007a). This concept involves a passive radar receiver placed inside a near-space platform is in conjunction with the illuminator of opportunistic signals, so as to provide persistent homeland mapping and monitoring. More importantly, rather than

emitting signals, this imaging system relies on the illuminators of opportunistic signals. This is particularly attractive, because it is desirable for such sensor to serve also other purposes like disaster monitoring, traffic monitoring and weather prediction. The remaining sections of this paper are organized as follows. In Section 2, the system concept of near-space remote sensing is presented, followed by the possibility analysis in Section 3. Next, the potentials and challenges are investigated in Section 4 and Section 5, respectively. Finally, Section 6 concludes the whole paper.

2. SYSTEM CONCEPT

As an example, we take the global navigation satellite systems (GNSS) signals as the opportunistic signals. The use of GNSS has many advantages such as entire planet coverage, simple transmitter -receiver synchronization, and precise knowledge of the transmitter spatial information. Some applications have surfaced, but the application of this technique to homeland security was mostly ignored or overlooked.

The passive receiver consists two channels. One channel is fixed to collect the signal arriving at the receiver travelling directly from the GNSS transmitters. This signal can be used as the reference signal for matched filtering, and referred to as $x_d(t)$. The second channel is configured to gather the scattered signal, and referred to as $x_s(t)$. This signal is sampled in a delay window that can be predicted using the knowledge of the near-space receiver, along with that of the GNSS transmitter and surface elevation. For homeland security applications, the GNSS signal reflection or scattering by an object is based on its surface reflectivity, which is the ratio of the reflected power to direct power. This configuration is of great interest because it

offers two significant advantages over current spaceborne /airborne radar systems. The first advantage is persistent region coverage, because the passive near-space platforms can provide stay-and-stare persistence for days, months, and even years. The second advantage is the potentials of bistatic radar configuration.

Although the receiver is stationary, an aperture synthesis can still be achieved by the motion of GNSS satellites (He, et al., 2005). As SAR (synthetic aperture radar) images are usually derived through correlation of the raw data with a two-dimensional reference function. Here the range resolution is achieved by measuring the correlation power between $x_d(t)$ and $x_r(t)$.

Similarly, azimuth resolution is obtained by exploiting the relative motion between the GNSS transmitter and the target, which leads to the target returns having a Doppler bandwidth. Additionally, the configuration using a single receiver is also feasible. In this case, the received signal would contain the signals from both the direct-path channel and the scattered channel. Once they are separated, successful matched filtering can still be achieved.

3. FEASIBILITY ANALYSIS

Using GNSS transmitter as an illuminator for near-space passive remote sensing presents a problem of signal detectability because the received signal will be very weak. As such, signal detectability is investigated in this section.

3.1 Detectable Range

The power of the target reflection available at the near-space receiver antenna output is determined by

$$P_r = \frac{P_t G_t}{4\pi R_t^2} \cdot \frac{\sigma_o}{4\pi R_r^2} \cdot \frac{\lambda G_r}{4\pi} \quad (1)$$

where P_t is the transmitted power, G_t is the transmitter antenna gain, R_t is the transmitter-to-target distance, σ_o is the radar cross section (RCS), R_r is the target-to-receiver distance, λ is the wave-length and G_r is the receiver antenna gain, respectively. The power flux density near the Earth's surface produced by GNSS can be assumed to be $P_t G_t / 4\pi R_t^2 = \Pi_0 \approx 3 \cdot 10^{-14} \text{ Wt} / \text{m}^2$. The noise level at the output of the RF front-end can be represented by

$$N_0 = K T_0 B_w \quad (2)$$

where K , T_0 and B_w are the Boltzmann constant, system noise temperature and noise bandwidth, respectively. Hence, with the consideration of processing gain G_{sp} , the signal-to-noise ratio depends on

$$SNR_r = \frac{P_r}{N_0} = \Pi_0 \cdot \frac{\sigma_o}{4\pi R_r^2} \cdot \frac{\lambda^2 G_r}{4\pi K T_0 B_w} \cdot G_{sp} \quad (3)$$

Thus, the detectable maximum range can be expressed as

$$R_{\max} = \sqrt{\Pi_0 \cdot \frac{\sigma_o}{4\pi} \cdot \frac{\lambda^2 G_r}{4\pi K T_0 B_w} \cdot \frac{G_{sp}}{SNR_{\min}}} \quad (4)$$

and the maximum sensitivity is determined by

$$SNR_{\min} = \frac{K T_0 N_0 \gamma_0}{\tau_p} \quad (5)$$

where γ_0 is a constant parameter, and τ_p is the coherent integration time.

As an example, assuming the following parameters: $\Pi_0 = -130 \text{ dBW} / \text{m}^2$, $\sigma_o = 20 \text{m}^2$, $\lambda = 0.19 \text{m}$, $G_r = 36 \text{dB}$, $T_0 = 300$, $B_w = 2.4 \text{MHz}$, $G_{sp} = 65 \text{dB}$, $SNR_{\min} = 0 \text{dB}$, then R_{\max} is found to be 24.01km. This value validates that the requirement of power budget is satiable. Notice that R_{\max} can be further increased by increasing the effective area of the receiver antenna.

3.2 Signal-to-Noise Ratio

For radar image formation, the total data samples are processed coherently to produce a single image resolution cell. The thermal noise samples can be taken as independent from sample to sample within each pulse, and from pulse to pulse. After coherent range and azimuth compression, the image signal-to-noise ratio (SNR) is given as (He, et al., 2005)

$$SNR_{\text{image}} = \Pi_0 \cdot \frac{A_r \sigma_o}{4\pi R_r^2} \cdot \frac{1}{K T_0 F_n} \cdot \frac{R_r}{v_s \cdot \rho_a} \cdot \eta \quad (6)$$

where A_r , F_n , v_s and η are the effective area of the receiver antenna, noise figure, satellite velocity and loss factor, respectively. As the potential azimuth resolution can be rewritten as

$$\rho_a = \frac{\lambda R_t}{L_s} = \frac{\lambda R_t}{v_s T_s} \quad (7)$$

with T_s the integration time, we can get

$$SNR_{\text{image}} = \frac{\Pi_0 A_r \sigma_o T_s \eta}{4\pi R_r^2 F_n K T_0} \quad (8)$$

As an example, assuming a typical system with the following parameters: $\sigma_o = 20 \text{m}^2$, $T_s = 1000 \text{s}$, $T_0 = 300$, $\eta = 0.5$, and $F_n = 2 \text{dB}$, then the calculated SNR is illustrated in Fig. 1. Here the SNR is favourable owing to an essentially long integration time. Note that this SNR can be further improved by using non-coherent integration of signals from more than one receiver channel.

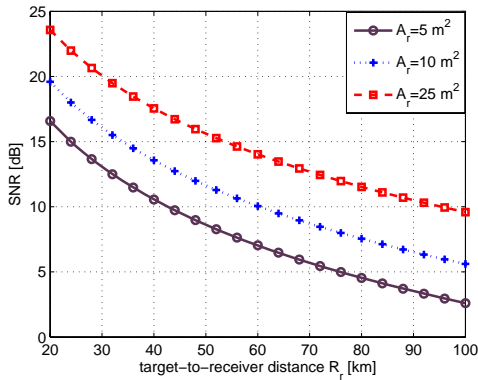


Figure 1: Power budget analysis of SNR

3.3 Noise Equivalent Sigma Zero

A quantity directly related to radar image performance is the noise equivalent sigma zero (NESZ). The NESZ is the mean RCS necessary to produce a SNR_{image} of unity. The NESZ can be interpreted as the smallest target cross section which is detectable by the SAR system against thermal noise. Setting $SNR_{image} = 1$, Eq. (8) gives

$$NESZ = \frac{4\pi R_r^2 F_n K T_0}{\Pi_0 A_r T_s \eta} \quad (9)$$

Assuming again the same parameters as the last section, the calculated NESZ is illustrated in Fig. 2. This results clearly show that a comparable RCS requirement to current radar systems is possible.

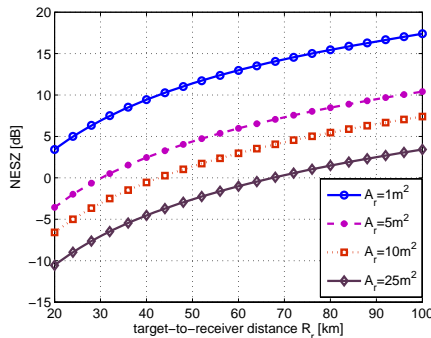


Figure 2: Power budget analysis of NESZ

3.4 Cluster Power Estimate

Another consideration is clutter, which can be assumed to enter the system via the antenna sidelobes only. Take GPS as an example, the transmitted signal is a spread spectrum system with a chip rate of 1.023M Hz, the clutter power at the receiver antenna can be represented by

$$P_c = \Pi_0 \cdot \frac{\sigma_c}{2} \cdot \log\left(1 + \frac{\rho_r}{R_r}\right) \cdot \frac{\lambda^2 G_{sl}}{4\pi} \quad (10)$$

where σ_c and G_{sl} are the RCS of the clutter per unit area and the sidelobe gain of the antenna, respectively. From radar equation we get the clutter-to-target power ratio (CTPR) as

$$CTPR = \frac{P_c}{P_r} = 2\pi \cdot \frac{\sigma_c}{\sigma_0} \cdot \frac{G_{sl}}{G_r} \cdot R_r^2 \cdot \log\left(1 + \frac{\rho_r}{R_r}\right) \quad (11)$$

To estimate the clutter power, we suppose that $G_{sl} = -10dB$, $\sigma_c = -20dB$, and the other parameters are same as the last sections. Figure 3 gives the clutter-to-target power ratio for different values of R_r and A_r ($A_r = \lambda^2 G_r / 4\pi$). The results show that the clutter contains almost as much as power as the target returns. This situation can be improved by reducing the magnitude of the antenna sidelobe gain or the application of space-time adaptive signal processing algorithms, e.g., fractional Fourier transform. Moreover, the CTPR can be further improved owing to subsequent range compression and azimuth compression.

4. POTENTIALS

In this section, we addressed the potential analysis of near-space passive remote sensing for homeland security applications, while compared with spaceborne and airborne remote sensing.

4.1 Persistent Coverage

Due to the unavoidable consequences of orbital mechanics, a satellite at other than GEO altitudes cannot remain within view of an area indefinitely. Generally speaking, air-breathing aerodynamically lifted platforms cannot routinely operate much above 18.3km. Similarly satellites usually operate in the orbits

above 200km, otherwise tenuous atmospheric drag will significantly reduce their lifetimes. As a result, physical limitations due to orbital mechanics and fuel consumption prevent a persistent coverage for current radars. Fortunately this can be achieved through the use of near-space free-floaters flying in the region where the prevailing winds are relatively mild because it is above storms and jet steam. Being defined as the region between 20km and 100km, near-space offers a number of benefits, but the most promising is persistence.

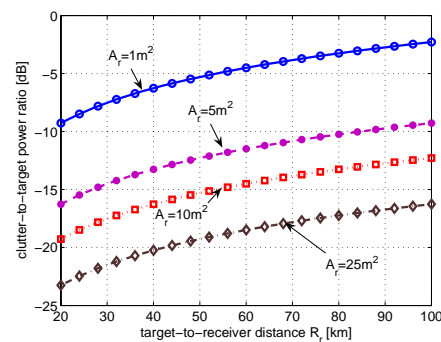


Figure 3: Calculated clutter-to-target power ratio.

The lower limit of near-space is not only determined from operational considerations, being above controlled airspace, but meteorological one as well. The 20km altitude is above the troposphere, the atmosphere region where most weather occurs. There are no clouds, thunderstorms, or precipitation in near-space. In fact, there is a region in near-space where average winds are less than 20 knots, with peak winds being less than 45 knots for 95 percent of the time.

4.2 Robust Survivability

Near-space free-floaters are inherently survivable. They have extremely small RCS (radar cross section) making them relatively invulnerable to most traditional tracking and locating methods. Estimates of their RCS are as small as that of a bird (Tomme, 2005), and as a result currently documented radars are unable to find them. At this altitude the acquisition and tracking will be technical challenges even without considering what sort of weapon could reach them since few weapons are designed to engage a target with very low RCS. Even if the acquisition and location problems are overcome, near-space assets are still difficult to be destroyed. The way they are manufactured has a lot to do with their relative invulnerability. Near-space free-floaters can be manufactured in two basic types: super-pressure and zero-pressure. Super-pressure ones are inflated and sealed, much like a child's toy helium balloon. Zero-pressure ones have venting system that ensures the pressure inside the balloon is same as the surrounding atmosphere. The second kind is less vulnerable to puncture. Imaging an inflated, lightweight plastic garment bag floating on the wind; even if there are many small holes in such a bag, it still can float in the air for a long time.

4.3 Bistatic Observation

Bistatic observation can provide many specific advantages, like the exploitation of additional bistatic information (Kuang and Jin, 2007), reduced vulnerability in military systems (Wang and Cai, 2007b), and improved detection capability of slowly moving targets (Li, et al., 2007). Objects detection in heterogeneous environments, e.g., homeland security, will further take advantage of reduced retro-reflector effects (Fernandez, et al., 2006). The segmentation and classification of natural surface and volume scatterers are alleviated by comparing the spatial statistics of mono- and bistatic scattering coefficients. Bistatic observations may also increase the RCS of manmade objects and/or the sensitivity to specific scattering centres of objects composites. Furthermore, bistatic observation in a forward scattering geometry have also great potential for systematic vegetation monitoring. Homeland monitoring will take advantage of the specular coherent reflection, which enables more sensitive object estimates over a wider dynamic range with lower saturation.

4.4 Low Cost

When cost is the concern, near-space has no peer. Their inherent simplicity, recoverability, relative lack of requirement for complex infrastructure, and lack of space-hardening requirements all contribute to this strong advantage for assets. Requiring only helium for lift, near-space platforms do not require expensive space launch to reach altitude. If the payloads they carried have malfunction, they can be brought back down and repaired. When they become obsolete, they can be easily replaced. Not being exposed to the high levels of radiation common to the space environment, payloads flown in near-space require no costly space-hardening manufacture.

Additionally, operating in near-space obviously eliminates a great deal of expense involved in space sensor construction. The infrastructure cost savings involved with near-space are huge. Near-space platforms require extremely minimal launch infrastructure. Only a simple tie-down and an empty fielded are required, but a space-launch complex or even a hard-surface runway must be built for satellites and airplanes.

5. CHALLENGES

5.1 Synchronization Techniques

The near-space remote sensing discussed in this paper is a bistatic configuration, it is subject to the problems and special requirements that are either not encountered or encountered in less serious form for current monostatic SAR systems. The biggest challenge lies in the synchronization between the near-space receiver and the GNSS satellites: phase synchronization, the near-space receiver and the GNSS satellites must be coherent over extremely long periods of time; spatial synchronization, the near-space receiving antenna and the GNSS transmitting antennas must simultaneously illuminate the same spot on the ground.

There is no cancellation of low-frequency phase noise as in a monostatic radar, where the same oscillator is used for modulation and demodulation. We can express the synchronization errors as

$$\phi_e = \int_0^{\Delta T} 2\pi(f_t - f_r)dt \quad (12)$$

where f_t and f_r denote the GNSS transmit carrier frequency and near-space receive demodulation frequency, respectively, ΔT is the integrated time and should be greater than one aperture time. A typical requirement for the maximum tolerable ISLR (integrated sidelobe ratio) is -20dB . Unfortunately, the phase synchronization errors are usually random and too complex to apply autofocus algorithms.

As shown in Fig. 4 for four point targets, it is evident that oscillator phase noise may not only defocus the radar image, but also introduce significant positioning errors along the scene extension, so some synchronization technique or compensation algorithms must be applied. One possible solution is the direct-path signal based synchronization technique (Wang, et al., 2008). However notice that, although the feasibility of general bistatic radar concept was already demonstrated by experimental investigations, the synchronization including time, spatial and phase is still the primary impediment to current bistatic radar development in general, not only to the near-space passive bistatic radar discussed in this paper.

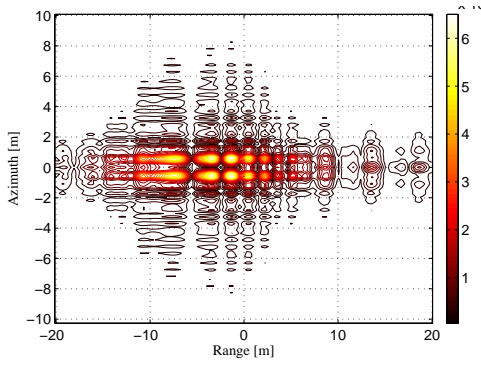


Figure 4: Impact of phase synchronization errors

5.2 Bistatic Radar Processing

Another challenge is bistatic radar processing. As a starting point, most radar imaging algorithms are assumed that the transmitted signal is a chirp signal, this is not the case for a GNSS signal. Moreover, as the GNSS transmitter follows a rectilinear trajectory, while the receiver remains in a fixed position on a near-space platform looking down to the illuminated scene. This configuration with fixed receiver also brings some challenges on image formation algorithms. The instantaneous slant range of a given target as a function of its geometry is

$$R(t_{az}) = \sqrt{R_{r0}^2 + v^2 \cdot (t_{az} - t_{dc})^2} + \sqrt{R_{r0}^2 + v^2 \cdot t_{dc}^2} \quad (13)$$

where t_{az} and t_{dc} are the azimuth time and the time while the target at the beam center crossing, respectively. R_{r0} is the slant range of closest approach to the transmitter, and R_{r0} that to the receiver which moves in a path parallel to the transmitter.

It can be noticed that the range history of a given point target does not depend any more only on the zero-Doppler distance and the relative distance from the target to the transmitter, but also on the absolute distance to the receiver. But the distance to the receiver is only a function of the coordinates R_{r0} and t_{dc} , and independent of the varying variable t_{az} . Then the Doppler chirp rate K_d can be derived from the instantaneous slant range as

$$K_d = \frac{d^2[R(t_{az})/\lambda]}{d(t_{az}^2)} \Big|_{t_{az}=t_{dc}} \approx \frac{v^2}{\lambda R_{r0}} \quad (14)$$

Hence the azimuth phase modulation of a target is due to the motion of the transmitter alone. As a consequence, there is a range ambiguity that does not exist in the monostatic case, i.e., two or more targets located at different positions can have the same range delay at zero-Doppler but will have different range histories. This complex signal model represents a great challenge towards the development of precise and efficient focusing algorithms. One effective algorithm is non-linear chirp scaling (NLCS), as shown in Fig. 5. H_1 is a chirp scaling factor which makes the range cell migration (RCM) of all targets along the swath be the same, can be expressed as

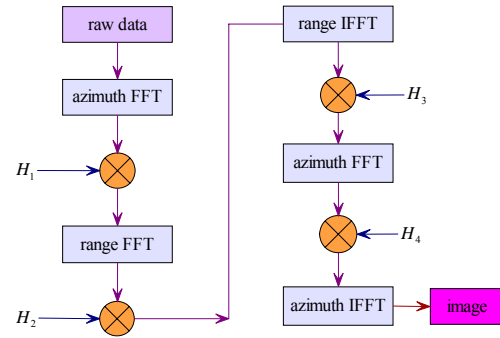


Figure 5: Block scheme of signal processing algorithm.

$$H_1(t, f_a; R_{t0}) = \exp \left\{ -j\pi k_r \left[\frac{1}{\sqrt{1 - \left(\frac{\lambda f_a}{v} \right)^2}} - 1 \right] \times \left(t - \frac{R(f_a; R_{t0})}{c} \right)^2 \right\} \quad (15)$$

where k_r , λ , f_a , v , $R(f_a; R_{t0})$ and c denote the range chirp rate, signal wavelength, instantaneous Doppler frequency, GNSS transmitter velocity, range in range-Doppler domain and light speed, respectively. After range chirp scaling, a range processing factor

$$H_2(f_r, f_a; R_{t0}) = \exp \left\{ j \left[\frac{\pi R_{t0} \lambda^2 f_a^2 f_r}{c v^2} + \frac{\pi f_r^2}{k_r(f_a; R_{t0})} \right] \right\} \quad (16)$$

is applied to the two-dimensional frequency-domain signal, which completes the range compression and bulk RCM correction. This makes the Doppler chirp rate changes with the azimuth position in the same range gate.

To perturb their Doppler chirp rate to be the same, we use one perturbation factor (Wong and Yeo, 2001)

$$H_3(\tau_{az}) = \exp \left[j\pi \frac{v^2}{\lambda} \left(\frac{\alpha_1}{6} \tau_{az}^4 + \frac{\alpha_2}{15} \tau_{az}^6 + \frac{\alpha_3}{28} \tau_{az}^8 \right) \right] \quad (17)$$

where α_1 , α_2 and α_3 are constant coefficients. Finally, the azimuth Doppler chirp rate corrected azimuth-time domain signal can be azimuth compressed with the following reference function

$$H_4(f_a; R_{t0}) = \exp \left[j\pi \frac{\lambda R_{t0} f_a^2}{v^2} \right] \quad (18)$$

In this way, focused radar image can be achieved. However, this situation will become more complicated for unflat DEM

(digital elevation model) topography. Note that, in monostatic radar, the scene topography is not considered in the focusing algorithms because the measured range delay is directly related with the double target distance and the observed range curvature. Therefore, some new imaging algorithms should be developed for near-space passive remote sensing.

5.3 Motion Compensation

For many creative applications of near-space passive radar, strict relative position or altitude is required. In this paper, we suppose the near-space platform is stationary. However, as a matter of fact, problems arise due to the presence of atmospheric turbulence, which introduce aircraft trajectory deviations from the nominal position, as well as altitude (roll, pitch, and yaw angles). For current radar systems, the motion compensation is usually achieved with GPS and INU (Inertial Navigation Units). However, for near-space passive remote sensing the motion measurement facilities may be not reachable, the conventional motion sensors based motion compensation techniques may be not applicable any longer, so some new efficient motion compensation algorithms must be developed. To reach this aim, we can use the transponder proposed by (Weiβ, 2002), as shown in Fig. 6, to extract the motion compensation information.

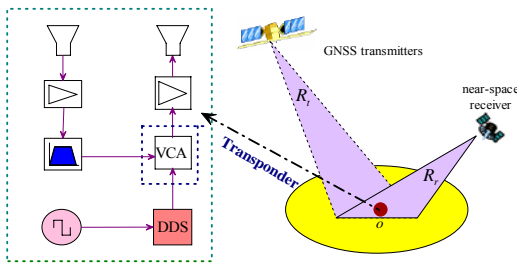


Figure 6: Transponder based motion compensation.

This transponder consists of a low-noise amplifier followed by a bandpass filter. A voltage controlled attenuator (VCA) is used to modulate the radar signal in a manner that the retransmitted signal will show two additional Doppler frequencies. Thereafter the signal will be amplified to an appropriate level and retransmitted towards the near-space receiver. This transponder can be seen as an amplitude modulator, that is

$$s_c(t) = [\alpha + \beta \cos(2\pi f_m t + \varphi_m)] \cdot s_0(t) \quad (19)$$

with f_m is the modulation frequency of transponder, φ_m the starting phase and $s_0(t)$ the GNSS transmitted signal. We can notice that, the retransmitted signal will show the original GNSS signal and two additional Doppler frequencies, one positive and one negative shifted, allowing to extract the motion compensation information without clutter interferences.

The corresponding near-space sensor received signal can be represented by

$$s_r(t) = s_s(t) + [\alpha + \beta \cos(2\pi f_m t + \varphi_m)] \cdot s_m(t) \quad (20)$$

where $s_s(t)$ and $s_m(t)$ denote the un-modulated part and the

echo of the transponder without the amplitude modulation, respectively. After applying a Fourier transform to Eq. (20), we have

$$S_r(f) = S_s(f) + \alpha S_m(f) + \frac{\beta}{2} e^{-j\varphi_m} S_m(f + f_m) + \frac{\beta}{2} e^{j\varphi_m} S_m(f - f_m) \quad (21)$$

The upper and lower side bands of this signal can be acquired using appropriate filters. Notice that, the filter bandwidth has to be chosen according to the signal bandwidth of $s_m(t)$ and the frequency distance between the clutter and the modulation frequency f_m . If let

$$\begin{cases} S_a(f) = \frac{\beta}{2} e^{j\varphi_m} S_m(f - f_m) \\ S_b(f) = \frac{\beta}{2} e^{-j\varphi_m} S_m(f + f_m) \end{cases} \quad (22)$$

The starting phase φ_m can be calculated as

$$S_a(f + f_m) \cdot S_b^*(f - f_m) = \beta e^{i2\varphi_m} \quad (23)$$

modulo π . Using this starting phase, the transponder signal can be calculated by

$$S_m(f) = \frac{[S_a(f + f_m) e^{-j\varphi_m} + S_b(f - f_m) e^{j\varphi_m}]}{\beta} \quad (24)$$

Thereafter, $S_m(f)$ can be transformed back into its time representation $s_m(t)$ using an inverse Fourier transform. Evaluation of the phase of $s_m(t)$ leads to a motion compensation solution. Note that another possible motion compensation solution is raw data based autofocus algorithms. We plan to carry out further investigation on this topic during subsequent work.

6. CONCLUSION

Near-space can provide many functions more responsively and more persistently than satellite and airplane for several reasons. First, it can support uniquely effective and economical operations. Second, it enables a new class of especially useful intelligence data. And finally, it provides a crucial corridor for prompt global strike. Inspired by recent advances in near-space technology, this paper presented the system concept of near-space passive remote sensing for homeland security applications. The novelty of this paper is the application of near-space remote sensing to homeland monitoring and to related applications. When one understands that it is effects instead of the platform from which the effects are delivered, near-space makes much sense for homeland security applications. Note that there are many other possible applications, e.g., disaster monitoring. Recently the frequency

of natural disasters has shown rapid increase. Examples of this trend are related to floods, earthquakes, tsunamis, hurricanes and forest fires (Tralli, et al., 2005). Methods and strategies have to be developed to predict as well as to tackle the natural disasters. It is shown that near-space does indeed offers a significant opportunity for homeland security applications, and no other way existed can provide similar effects. Issues have been highlighted, but there are clear paths of future work such as synchronization, signal detection, imaging algorithms and motion compensation to overcome them. The concepts and techniques investigated in this paper may be regarded as the Phase I work towards promising near-space passive remote sensing for homeland security applications. Although exploring the potential of near-space passive remote sensing missions requires significant work on many fronts, we are indeed convinced the effort will be worth it.

ACKNOWLEDGEMENTS

This work was supported in part by the Open Fund of the Key Laboratory of Ocean Circulation and Waves, Chinese Academy of Sciences under Contract number **KLOCAW0809**; and supported in part by the Open Fund of the Beijing Key Lab of Spatial Information Integration and 3S Application, Peking University under Contract number **SIIBKL08-1-04**.

REFERENCES

- Baker, C. J. and Griffiths, H. D., 2005. Bistatic and multistatic radar sensors for homeland security. *Advances in with Security*
- Trouve, E., Vasile, G. and Gay, M., 2007. Combining airborne photographs and spaceborne SAR data to monitor temperate ciers: potentials and limits. *IEEE Transactions on Geoscience and Remote Sensing* **45**, pp. 905–924.
- Wang, W. Q., 2007. Application of near-space passive radar for homeland security. *Sensing and Imaging: An International Journal* **8**, pp. 39–52.
- He, X., Cherniakov, M. and Zeng, T., 2005. Signal detectability in SS-BSAR with GNSS non-cooperative transmitter. *IEE Proceedings -Radar Sonar and Naivigation* **152**, pp. 124–132.
- Tomme, E. B., 2005. The paradigm shift to effects-based space: near – space as a common space effects enabler. <http://www.airpower.au.af.mil>, access in Oct. 2006.
- Kuang, K. and Jin, Y. Q., 2007. Bistatic scattering from a three-dimensional object over a randomly rough surface using the FDTD algorithm. *IEEE Transactions on Antennas and Propagation* **55**, pp. 2302–2312.
- Wang, W. Q. and Cai, J. Y., 2007. A technique for jamming bi-and multistatic SAR systems. *IEEE Geoscience and Remote Sensing Letters* **4**, pp. 80–82.
- Li, G., Xu, J., Peng, Y.N. and Xia, X. G., 2007. Bistatic linear antenna array SAR for moving target detection, location, and imaging with two passive airborne radars. *IEEE Transactions on Geoscience and Remote Sensing* **45**, pp. 554–565.
- Fernandez, P. D., Cantalloube, H., Vaizan, B., Krieger, G., Horn, R., Wendler, M. and Giroux, V., 2006. ONERA-DLR SAR bistatic campaign: planning, data acquisition, and first analysis of bistatic scattering behaviour of natural and urban targets. *IEE Proceedings -Radar Sonar and Navigation* **153**, pp. 214–223.
- Wang, W. Q., Ding, C. B. and Liang, X. D., 2008. Time and phase synchronization via direct-path signal for bistatic synthetic aperture radar systems. *IET Radar Sonar and Navigation* **2**, pp. 1–11.
- Wong, F.H. and Yeo, T.S., 2001. New application of nonlinear chirp scaling in SAR data processing. *IEEE Transactions on Geoscience and Remote Sensing* **39**, pp. 946–953.
- Wei, M., 2002. A new transponder technique for calibrating wideband imaging radars. *Proc. of Europe Synthetic Aperture Radar Conference, Germany*, pp. 493–495.
- Tralli, D.M., Blom, R.G., Zlotnicki, V., Donnellan, A. and Evans, D.L., 2005. Satellite remote sensing of earthquake, volcano, flood, landslide and coastal inundation hazards. *ISPRS Journal Photogrammetry Remote Sensing* **59**, pp. 185–198. Applications, Ciocco, Italy, pp. 1–22.

